UCRL 3572
c.2

UNIVERSITY OF CALIFORNIA

Radiation Laboratory

TWO-WEEK LOAN COPY

This is a Library Circulating Copy which may be borrowed for two weeks. For a personal retention copy, call Tech. Info. Division, Ext. 5545

BERKELEY, CALIFORNIA

DISCLAIMER

This document was prepared as an account of work sponsored by the United States Government. While this document is believed to contain correct information, neither the United States Government nor any agency thereof, nor the Regents of the University of California, nor any of their employees, makes any warranty, express or implied, or assumes any legal responsibility for the accuracy, completeness, or usefulness of any information, apparatus, product, or process disclosed, or represents that its use would not infringe privately owned rights. Reference herein to any specific commercial product, process, or service by its trade name, trademark, manufacturer, or otherwise, does not necessarily constitute or imply its endorsement, recommendation, or favoring by the United States Government or any agency thereof, or the Regents of the University of California. The views and opinions of authors expressed herein do not necessarily state or reflect those of the United States Government or any agency thereof or the Regents of the University of California.

UCRL-3572

UNIVERSITY OF CALIFORNIA
Radiation Laboratory
Berkeley, California

Contract No. W-7405-eng-48

PHOTON SCATTERING FROM PROTONS AND DEUTERONS

R. H. Capps

October 30, 1956

Printed for the U. S. Atomic Energy Commission

PHOTON SCATTERING FROM PROTONS AND DEUTERONS

R. H. Capps

Radiation Laboratory
University of California
Berkeley, California

October 30, 1956

ABSTRACT

The scattering of photons of 100 to 200 Mev from protons and deuterons is examined in a model in which it is assumed that only electric and magnetic dipole photons scatter. Two dispersion relations derived by Gell-Mann, Goldberger, and Thirring, and the analysis of photopion production from nucleons by Watson, Keck, Tollestrop, and Walker, are used to guide the theoretical prediction of differential scattering cross sections. Several approximations are made, including the impulse approximation in the discussion of photon-deuteron scattering; the accuracy of these approximations is estimated. In this model the photon-proton cross section, and the sum of the elastic and inelastic photon-deuteron cross sections are largest at backward scattering angles. Several feasible types of photon-deuteron scattering experiments are discussed briefly.

PHOTON SCATTERING FROM PROTONS AND DEUTERONS

R. H. Capps

Radiation Laboratory
University of California
Berkeley, California

I. INTRODUCTION

Photons of energy in the range 100 to 300 Mev may be used to probe the pionic structure of nucleons and of complex nuclei. In the past few years many laboratories have attacked the problem of measuring the elastic scattering of high-energy photons from nuclei;[1,2,3,4] progress has been slow, however, because the photon-nucleon scattering cross section is extremely small, on the order of $(e^2/Mc^2)^2 \approx 1.5 \times 10^{-32}$ cm^2/steradian. Experimental cross sections for high-energy photon scattering from various nuclei are known at present only vaguely, though it appears that the measurements may be improved significantly in the next few years.

Two different models of photon-proton scattering predict that the pionic contributions to the differential cross section should be small at energies below 100 Mev and should increase rapidly in the energy range 100 to 150 Mev.[5,6] The experiments of Oxley and Telegdi[2] tend to support the conclusion that the 100-Mev cross section differs by little from the prediction of the Klein-Nishina formula modified by the inclusion of the

---

1 Pugh, Frisch, and Gomez, Phys. Rev. 95, 950 (1954).

2 C. L. Oxley and V. L. Telegdi, Phys. Rev. 100, 435 (1955).

3 Gomez, Pugh, Frisch, and Janes, Phys. Rev. 100, 1245 (1955).

4 Janes, Gomez, Pugh, and Frisch, Phys. Rev. 100, 1245 (1955); Larry Higgins and Burton J. Moyer (private communication); several other groups have also worked on this problem.

5 Gell-Mann, Goldberger, and Thirring, Phys. Rev. 95, 1612 (1954). This paper (and its authors) will be referred to by the symbols GGT.

6 R. H. Capps and W. G. Holladay, Phys. Rev. 99, 931 (1955).

Pauli anomalous moment. Pionic effects are important for energies greater than 150 Mev also; however, the experimental measurement is more difficult in this region because of the background of high-energy gamma rays produced in the decay of photoproduced neutral pions. Since the energy resolution of present gamma-ray detectors is not very sharp (about 30 Mev), the neutral-pion-production events may be separated from scattering events only if the angle or energy (or both) of the recoiling nucleon is measured with a fair degree of accuracy. Above 150 Mev the theoretical analysis also is more complicated because recoil effects and effects of high angular momenta are more important than at lower energies. In this work we shall concentrate primarily on the energy range 100 to 190 Mev since pionic effects should be noticeable in this region, yet the experimental and theoretical treatment is not excessively complicated.

Since pure neutron targets are not available, one can determine the photon-neutron cross section only by analyzing the results of scattering from complex nuclei. Such an analysis can be made in a simple manner if the impulse approximation[7] is valid for this process. The deuteron represents the most suitable nucleus for application of the impulse approximation, since the average separation between the proton and neutron is relatively large, and the deuteron wave function is known fairly accurately. In Sections III and IV of this paper possible photon-deuteron scattering experiments are discussed, and the validity of the impulse approximation is estimated.

---

[7] G. F. Chew, Phys. Rev. 80, 196 (1950); G. F. Chew and M. L. Goldberger, Phys. Rev. 87, 778 (1952). Several references to previous works on the impulse approximation are given in the work by Chew and Goldberger.

The theoretical prediction of photon-proton and photon-deuteron scattering is greatly facilitated by the use of dispersion relations. Gell-Mann, Goldberger, and Thirring (GGT) have derived dispersion relations for the spin-independent and spin-dependent forward photon-nucleon amplitudes, and have showed that the spin-independent forward amplitude (the coherent amplitude) may be determined to a high degree of accuracy from a knowledge of the behavior as a function of energy of the total cross section for production of pions by an unpolarized beam of photons.[5] Since the publication of GGT many authors have derived various dispersion relations for pion-nucleon scattering.[8] It appears that the various techniques used in these works, if applied to photon-nucleon scattering, may enable one to determine approximately the differential cross sections at all angles from a knowledge of the dependence on energy and angular momentum of the photopion-production cross sections. The analysis of Watson et al. has shown that two mechanisms predominate in the photoproduction from nucleons of pions at energies less than 400 Mev; first, the production of an S-wave pion by an electric dipole photon, and second, the production of a P-wave pion in a state of total angular momentum 3/2 by a magnetic dipole photon.[9] Thus, our present knowledge justifies the use of two separate dispersion relations in the prediction of the photon-nucleon scattering cross sections. In this paper the two dispersion

---

[8] M. L. Goldberger, Phys. Rev. 99, 979 (1955); R. Oehme, Phys. Rev. 100, 1503 (1955) and Phys. Rev. 102, 1174 (1956); R. H. Capps and Gyo Takeda, Phys. Rev. 103, 1877 (1956). The work by Capps and Takeda contains many references to other works.

[9] Watson, Keck, Tollestrup, and Walker, Phys. Rev. 101, 1159 (1956).

relations derived in GGT and the analysis of photoproduction of Reference 9 are used to help make such a prediction. A dispersion relation is used for the further purpose of estimating corrections to the impulse approximation in photon-deuteron scattering.

The basic assumptions of the present model are that the dispersion relations are valid, and that only electric and magnetic dipole waves are important in photon-pion-nucleon phenomena at low energies. This latter assumption depends on the assumption that only S- and P-wave pions are important for low-energy pion-nucleon phenomena. In addition to these basic assumptions several approximations are made, such as the impulse approximation in the case of photon-deuteron scattering; the accuracy of these approximations is estimated.

II. SCATTERING FROM PROTONS

A. The Differential Cross Section

The forward amplitude for the scattering of gamma rays from protons in the laboratory system may be written in the form

$$T_\ell^f(k_\ell) = A_\ell(k_\ell)\underset{\sim}{e}\cdot\underset{\sim}{e}' + i\,B_\ell(k_\ell)\underset{\sim}{\sigma}\cdot\underset{\sim}{e}\times\underset{\sim}{e}' , \tag{1}$$

where $A_\ell(k_\ell)$ and $B_\ell(k_\ell)$ are complex functions of k_ℓ, the magnitude of the momentum of the incident photon. The vectors $\underset{\sim}{e}$ and $\underset{\sim}{e}'$ are the polarization vectors of the incident and scattered photons, and $\underset{\sim}{\sigma}$ is the spin operator of the proton. The subscript ℓ is used to denote amplitudes and momenta that are to be measured in the laboratory system. Gell-Mann, Goldberger, and Thirring[5] have shown that the amplitudes A_ℓ and B_ℓ satisfy the following dispersion relations:

$$\mathrm{Re}\left[A_\ell(k_\ell) - A_\ell(0)\right] = \frac{2k_\ell^2}{\pi}\,P\int_0^\infty dk_\ell'\,\frac{\mathrm{Im}\,A_\ell(k_\ell')}{k_\ell'(k_\ell'^2 - k_\ell^2)} , \tag{2}$$

$$\mathrm{Re}\left[B_\ell(k_\ell) - k_\ell B_\ell'(0)\right] = \frac{2k_\ell^3}{\pi}\,P\int_0^\infty dk_\ell'\,\frac{\mathrm{Im}\,B_\ell(k_\ell')}{k_\ell'^2(k_\ell'^2 - k_\ell^2)} . \tag{3}$$

The integral of Eq. (2) may be written in terms of the total cross section $\sigma_T(k_\ell')$ for unpolarized incident photons, if use is made of the optical relation,

$$\mathrm{Im}\,A_\ell(k_\ell) = (k_\ell/4\pi)\sigma_T(k_\ell) . \tag{4}$$

This relation is derived in Appendix A. For simplicity the constants $\hbar$ and c are taken to be unity in this paper.

In order that we may make a partial-wave expansion of the scattering amplitude, it is convenient to introduce the center-of-mass amplitudes $A(k)$ and $B(k)$, which are related to $A_\ell(k_\ell)$ and $B_\ell(k_\ell)$ by the equations

$$A(k) = (k/k_\ell)\, A_\ell(k_\ell)$$

and

$$B(k) = (k/k_\ell)\, B_\ell(k_\ell) \quad ,$$

where k is the center-of-mass value of the magnitude of the photon momentum. The amplitudes A, B, A_ℓ, and B_ℓ are related to the center-of-mass and laboratory differential cross sections in the forward direction for unpolarized gamma rays by the equations

$$d\sigma_\ell = |A_\ell|^2 + |B_\ell|^2$$

and

$$d\sigma = |A|^2 + |B|^2 \quad .$$

Since the threshold value of the scattering amplitude is given by the Thomson amplitude, i.e.,

$$A_\ell(0) = -e^2/m$$

where e and m are the proton charge and mass, Eq. (4) may be used to write Eq. (2) in the form

$$\frac{k_\ell}{k} \operatorname{Re} A(k) + \frac{e^2}{m} = \frac{k_\ell^2}{2\pi^2} P \int_0^\infty dk_\ell' \frac{\sigma_T(k)}{(k_\ell'^2 - k_\ell^2)} \quad . \tag{5}$$

Since the reactions $\gamma + p \rightarrow p + \pi^0$ and $\gamma + p \rightarrow n + \pi^+$ dominate whenever they are energetically possible, one may, to a high degree of accuracy, replace σ_T by the total cross section for photopion production by unpolarized photons when using Eq. (5) to determine $\operatorname{Re} A(k)$. In GGT,

Re A(k) is determined by this procedure; the authors then predict the differential cross section for gamma-proton scattering in the energy range 0 to 300 Mev on the basis of a knowledge of A(k) and some reasonable guesses as to the relative sizes of the phase shifts. This section is an extension of the GGT analysis, the principal differences being that the effects of the anomalous and intrinsic magnetic moments are included, and both Eq. (5) and (3) are used, together with the analysis by Watson et al.[9] of photoproduction, to fix the two parameters A(k) and B(k).

It is assumed that at energies less than 200 Mev the only electromagnetic waves significantly scattered are those of angular momentum one, the electric and magnetic dipole waves. This assumption seems reasonable in view of the facts that the energy is small compared to the proton rest energy, and that dipole photons are responsible for the important features of photopion production at energies less than 400 Mev. Both the electric and magnetic waves may couple to the spin of the photon to form waves of total angular momentum $\frac{1}{2}$ and 3/2. Conservation of angular momentum and parity prevents transitions between these four states; thus in this approximation the only nonvanishing elements of the center-of-mass scattering amplitude T are the diagonal elements. We will denote these by $T_{\frac{1}{2}}^{e\ell}$, $T_{3/2}^{e\ell}$, $T_{\frac{1}{2}}^{mg}$, and $T_{3/2}^{mg}$ where the superscripts $e\ell$ and mg denote electric and magnetic amplitudes. These amplitudes are related to the phase shifts δ_i (which are in general complex) by equations of the form

$$T_i = k^{-1} e^{i\delta_i} \sin \delta_i$$

where i denotes the parity and angular momentum. Since the phase shifts are of the order $(e^2 k/m) \approx 0.001$ for our problem, it is an excellent

approximation to replace the above expression by

$$T_i \approx k^{-1} \delta_i \tag{6}$$

Since, in the differential cross section for unpolarized particles, there is no interference between spin-dependent and spin-independent amplitudes, it is convenient to work with such amplitudes. We define electric and magnetic spin-independent and spin-dependent amplitudes by the equations

$$\begin{aligned}
A^{e\ell}(k) &= T_{3/2}^{e\ell}(k) + \tfrac{1}{2} T_{\frac{1}{2}}^{e\ell}(k) \quad , \\
A^{mg}(k) &= T_{3/2}^{mg}(k) + \tfrac{1}{2} T_{\frac{1}{2}}^{mg}(k) \quad , \\
B^{e\ell}(k) &= \tfrac{1}{2} T_{3/2}^{e\ell}(k) - \tfrac{1}{2} T_{\frac{1}{2}}^{e\ell}(k) \quad , \\
B^{mg}(k) &= \tfrac{1}{2} T_{3/2}^{mg}(k) - \tfrac{1}{2} T_{\frac{1}{2}}^{mg}(k) \quad .
\end{aligned} \tag{7}$$

It may be shown that the forward spin-independent and spin-dependent amplitudes, $A(k)$ and $B(k)$, are related to the amplitudes of Eqs. (7) by the equations,

$$\begin{aligned}
A(k) &= A^{e\ell}(k) + A^{mg}(k) \\
B(k) &= B^{e\ell}(k) + B^{mg}(k) \quad .
\end{aligned} \tag{8}$$

At low photon energies the electromagnetic field feels only the gross properties of the proton. It has been shown by several authors that, in a gauge-invariant and relativistically invariant theory, the first two terms in an expansion in powers of energy of the amplitude for scattering of a photon from a spin $\frac{1}{2}$ particle are determined by the

charge, mass, and anomalous moment $\lambda e/2m$ of the particle.[10] To order k the center-of-mass amplitude T is given by

$$T = -\frac{ke^2}{k_\ell m}\, \underset{\sim}{e}\cdot\underset{\sim}{e}' - \frac{ie^2}{2m^2}\,(2\lambda + 1)k\; \underset{\sim}{\sigma}\cdot\underset{\sim}{e} \times \underset{\sim}{e}'$$

$$+ \frac{ie^2}{2m^2}\,(\lambda + 1)^2\; \frac{\underset{\sim}{\sigma}\cdot(\underset{\sim}{e} \times \underset{\sim}{k}) \times (\underset{\sim}{e}' \times \underset{\sim}{k}')}{k}$$

$$+ \frac{ie^2}{2m^2}\,(\lambda + 1)\left[\frac{\underset{\sim}{e}\cdot\underset{\sim}{k}'\; \underset{\sim}{\sigma}\cdot\underset{\sim}{k}' \times \underset{\sim}{e}' - \underset{\sim}{e}'\cdot\underset{\sim}{k}\; \underset{\sim}{\sigma}\cdot\underset{\sim}{k} \times \underset{\sim}{e}}{k}\right], \qquad (9)$$

where $\underset{\sim}{k}$ and $\underset{\sim}{k}'$ are the momenta of the incident and scattered photons, respectively.[11] The last term of this expression involves magnetic quadrapole photons, and is neglected in the present dipole model. From the first three terms of Eq. (9) it is seen that the low-energy behavior of the amplitudes $A^{e\ell}$, A^{mg}, $B^{e\ell}$, and B^{mg} is given by

---

10 F. E. Low, Phys. Rev. 96, 1428 (1955); M. Gell-Mann and M. L. Goldberger, Phys. Rev. 96, 1433 (1955). A somewhat similar theorem applying to gamma scattering from complex, structured systems is given by R. H. Capps, Phys. Rev. 99, 926 (1955).

11 The analogous expression for the laboratory amplitude is given by Eq. (1.1) of Low, Reference 10. The sign of T in Eq. (9) is opposite to the sign of the amplitude discussed by Low; this is a matter of convention.

$$\frac{k_\ell}{k} A^{e\ell} \approx -\frac{e^2}{m} ,$$

$$\frac{k_\ell}{k} A^{mg} \approx 0 ,$$

$$\frac{k_\ell}{k} B^{e\ell} \approx -\frac{e^2}{2m^2} (2\lambda + 1)k_\ell \approx -.34 \frac{e^2}{m} \frac{k_\ell}{\mu} , \tag{10}$$

$$\frac{k_\ell}{k} B^{mg} \approx -\frac{e^2}{2m^2} (\lambda + 1)^2 k_\ell \approx .58 \frac{e^2}{m} \frac{k_\ell}{\mu} ,$$

where μ is the pion mass and λ is taken to be 1.79.

At energies above 100 Mev the scattering amplitude should be considerably modified by pionic structure effects. Since partial waves corresponding to $T_{\frac{1}{2}}^{e\ell}$ and $T_{3/2}^{mg}$ are dominant in low-energy photopion production, we follow GGT in neglecting such pionic structure modifications in $T_{\frac{1}{2}}^{mg}$ and $T_{3/2}^{e\ell}$. Then the four dipole amplitudes have the form

$$\frac{k_\ell}{k} T_{3/2}^{e\ell}(k) = \frac{e^2}{m} \left[-\frac{2}{3} - \frac{1}{3} \frac{k_\ell}{m} (2\lambda + 1) \right] ,$$

$$\frac{k_\ell}{k} T_{\frac{1}{2}}^{e\ell}(k) = \frac{e^2}{m} \left[-\frac{2}{3} + \frac{2}{3} \frac{k_\ell}{m} (2\lambda + 1) \right] + \frac{e^2}{m} \mathcal{E}(k) ,$$

$$\frac{k_\ell}{k} T_{3/2}^{mg}(k) = \frac{e^2}{m} \left[\frac{1}{3} \frac{k_\ell}{m} (\lambda + 1)^2 \right] + \frac{e^2}{m} \mathcal{M}(k) , \tag{11}$$

$$\frac{k_\ell}{k} T_{\frac{1}{2}}^{mg}(k) = \frac{e^2}{m} \left[-\frac{2}{3} \frac{k_\ell}{m} (\lambda + 1)^2 \right] .$$

The terms in square brackets in Eqs. (11) are the threshold terms, determined from Eq. (7) and (10), while the functions $\mathcal{E}(k)$ and $\mathcal{M}(k)$ represent

pionic structure effects that are to be determined from the photoproduction data. It should be noted that, in the present approximation, the amplitudes T_i, $A^{e\ell,mg}$, $B^{e\ell,mg}$, $\mathcal{E}$ and $\mathcal{M}$ are all real at energies below pion-production threshold.

In order that the second dispersion relation, Eq. (3), be useful Im B must be replaced by a quantity that has to do directly with the photopion production cross sections. To do this we define partial cross sections $\sigma_{3/2}$ and $\sigma_{\frac{1}{2}}$, which represent the contributions to the total cross section for unpolarized, dipole photons from total angular momentum states 3/2 and $\frac{1}{2}$ respectively. Thus we have

$$\sigma_T = \sigma_{3/2} + \sigma_{\frac{1}{2}} + \text{higher multipole contributions.} \tag{12}$$

It is shown in Appendix A that, in our dipole model, Im B is given by

$$\frac{k_\ell}{k} \operatorname{Im} B(k_\ell) = (k_\ell/4\pi)(\tfrac{1}{2}\sigma_{3/2} - \sigma_{\frac{1}{2}}) \quad . \tag{13}$$

If Eq. (13) is substituted into Eq. (3) and $B'(0)$ is replaced by its value computed from Eqs. (8) and (10), Eq. (3) becomes

$$\frac{k_\ell}{k} \operatorname{Re} B(k) - \frac{k_\ell e^2 \lambda^2}{2m^2} = \frac{k_\ell^3}{2\pi^2} P \int_0^\infty dk_\ell' \frac{\left[\frac{1}{2}\sigma_{3/2}(k') - \sigma_{\frac{1}{2}}(k')\right]}{k_\ell'(k_\ell'^2 - k_\ell^2)} \quad . \tag{14}$$

As with Eq. (5), only the photopion production contribution to $\sigma_{3/2}$ and $\sigma_{\frac{1}{2}}$ need be used in evaluating the integral of Eq. (14). It should be noted that if photopion production were a spin-independent process, the integral of Eq. (14) would vanish in our approximation, for an unpolarized beam of dipole photons may be shown to be 2/3 in the state $j = 3/2$ and 1/3

in the state $j = \frac{1}{2}$. Thus, if there were no spin dependence, $\sigma_{3/2}$ would be equal to $2\sigma_{\frac{1}{2}}$, and the integral in Eq. (14) would be zero.

Equations (8), (7), and (11) may be used to write $A(k)$ and $B(k)$ in terms of known constants and the functions $\mathcal{M}(k)$ and $\mathcal{E}(k)$. If these expressions for $\mathcal{M}$ and $\mathcal{E}$ are substituted into Eqs. (5) and (14), these two dispersion equations become

$$\frac{e^2}{m} \operatorname{Re}\left[\mathcal{M}(k) + \tfrac{1}{2}\mathcal{E}(k)\right] = \frac{k_\ell^2}{2\pi^2} P \int_0^\infty dk_\ell' \frac{\sigma_T(k')}{(k_\ell'^2 - k_\ell^2)} ,$$

$$\frac{e^2}{m} \operatorname{Re}\left[\tfrac{1}{2}\mathcal{M}(k) - \tfrac{1}{2}\mathcal{E}(k)\right] = \frac{k_\ell^3}{2\pi^2} P \int_0^\infty dk_\ell' \frac{\left[\frac{1}{2}\sigma_{3/2}(k') - \sigma_{\frac{1}{2}}(k')\right]}{k_\ell'(k_\ell'^2 - k_\ell^2)} . \tag{15}$$

If the analysis of photopion production of Reference 9 is used to determine σ_T, $\sigma_{3/2}$, and $\sigma_{\frac{1}{2}}$, and the integrals are numerically integrated, Eqs. (15) determine $\operatorname{Re}\mathcal{M}$ and $\operatorname{Re}\mathcal{E}$ as functions of the energy. The results of such a procedure are shown by the solid curves in Fig. 1.

The imaginary parts of $\mathcal{M}$ and $\mathcal{E}$ also may be determined from the photoproduction data. Taking the imaginary parts of Eqs. (11), we obtain

$$\operatorname{Im} T_{3/2}^{e\ell} = \operatorname{Im} T_{\frac{1}{2}}^{mg} = 0 ;$$

$$(k_\ell/k) \operatorname{Im} T_{\frac{1}{2}}^{e\ell} = (e^2/m)\,\mathcal{E} ;$$

$$(k_\ell/k) \operatorname{Im} T_{3/2}^{mg} = (e^2/m)\,\mathcal{M} .$$

If these equations are combined with Eqs. (7), (8), (4), and (13), the imaginary parts of $\mathcal{M}$ and $\mathcal{E}$ are given by

$$\frac{e^2}{m} \operatorname{Im}\left[\mathcal{M}(k) + \tfrac{1}{2}\mathcal{E}(k)\right] = \frac{k_\ell}{4\pi}\sigma_T(k) ,$$

$$\frac{e^2}{m} \operatorname{Im}\left[\tfrac{1}{2}\mathcal{M}(k) - \tfrac{1}{2}\mathcal{E}(k)\right] = \frac{k_\ell}{4\pi}\left[\tfrac{1}{2}\sigma_{3/2}(k) - \sigma_{\frac{1}{2}}(k)\right] . \tag{16}$$

The imaginary parts of $\mathcal{M}$ and $\mathcal{E}$, determined from Eqs. (16) and the photoproduction data, are shown by the dashed curves in Fig. 1.

If the functions $\mathcal{M}(k)$ and $\mathcal{E}(k)$ are known, the amplitudes $A^{e\ell,mg}$ and $B^{e\ell,mg}$ may be determined from Eqs. (7) and (11). The differential cross section for unpolarized gamma rays may then be computed from Eq. (B3) of Appendix B. (The derivation of Eq. (B3) is discussed in Appendix B.) The center-of-mass, differential, "unpolarized" cross section, computed by the above procedure, is given in Fig. 2 at incident photon energies (in the lab system) of 120, 150, and 185 Mev.

Of the assumptions made in this section, perhaps the least justified is the assumption that the amplitudes $T_{3/2}^{e\ell}$ and $T_{\frac{1}{2}}^{mg}$ are given by their low-energy forms without pionic structure modifications. However, it does appear reasonable that such modifications are smaller than the corresponding modifications of $T_{\frac{1}{2}}^{e\ell}$ and $T_{3/2}^{mg}$. In the weak-coupling theory of Capps and Holladay[6] the ratio of the pionic structure modifications in the electric amplitudes $T_{\frac{1}{2}}^{e\ell}$ and $T_{3/2}^{e\ell}$ is about $\frac{1}{4}$ at 150 Mev. In terms of the present model this ratio R may be written

$$R = \frac{(k_\ell/k)T_{3/2}^{e\ell} - (e^2/m)\left[-\frac{2}{3} - \frac{1}{3}(k_\ell/m)(2\lambda + 1)\right]}{(k_\ell/k)T_{\frac{1}{2}}^{e\ell} - (e^2/m)\left[-\frac{2}{3} + \frac{2}{3}(k_\ell/m)(2\lambda + 1)\right]} . \tag{17}$$

In order to test the effect of a pionic structure modification in the

amplitude $T_{3/2}^{e\ell}$ we make the rather arbitrary assumption that the ratio of Eq. (17) is 1/3, and recalculate the differential cross section, corresponding to $k = 150$ Mev, again using Eq. (5) and (14) to determine the various amplitudes. The resulting cross section is shown in Fig. 3. It is seen that the most important characteristics of the cross section are not changed much by this assumption. The effect of a small but finite value of the ratio of Eq. (17) is even less pronounced at 120 and 185 Mev. The effect of a small finite value of $T_{\frac{1}{2}}^{mg}$ is also somewhat less than the corresponding effect for $T_{3/2}^{e\ell}$.

The differential cross sections may easily be converted to the laboratory system. To make this conversion one may use the relation

$$\int d\Omega \, d\sigma = \int d\Omega_\ell \, d\sigma_\ell ,$$

where the integrals are over corresponding solid angles, and the relation

$$d\Omega / d\Omega_\ell = (k_\ell'/k)^2 .$$

The laboratory differential cross sections corresponding to the center-of-mass cross sections of Fig. 2 are given in Fig. 4.

B. Comparison with Experiments and Other Theories

The results of high-energy gamma-proton scattering experiments[4] are not yet sufficiently conclusive to provide a test for the present model. From the analysis by the MIT group[1,3] of the scattering of 100- to 140-Mev photons from complex nuclei, there is some indication that the gamma-proton differential cross section is greater than (e^2/m) at $\theta = 135^\circ$, in agreement with the present model. This result is quite tentative, however,

because of the difficulties both in performing and in analyzing the experiment of scattering photons from complex nuclei.

It is instructive to compare the results of this paper with those of other theories. The front-back asymmetry in the 150-Mev differential cross section given here is similar to that predicted by GGT; the center-of-mass differential cross section of the present model increases from $0.1\ e^2/m$ to $3.1\ e^2/m$ as the scattering angle increases from 0° to 180°, while the corresponding cross section of GGT increases from $0.1\ e^2/m$ to $2.8\ e^2/m$ in the same range. The scattering amplitudes are quite different in the two theories, however. In the model of GGT the pionic structure modification of the amplitude $T_{3/2}^{mg}$ is larger than the corresponding modification of $T_{\frac{1}{2}}^{e\ell}$; the front-back asymmetry is caused by interference between the spin-independent part of $T_{3/2}^{mg}$ and the negative spin-independent electric dipole amplitude (the Thomson amplitude). In the present model the evaluation of the spin-dependent dispersion relation, Eq. (14), indicates that the magnetic modification $\mathcal{M}$ is smaller than the electric modification $\mathcal{E}$ at $k_\ell = 150$ Mev; thus the spin-independent magnetic amplitude is smaller than the corresponding amplitude of GGT. The front-back asymmetry in the spin-independent part $d\sigma_A$ of the differential cross section in Section IIA is only moderately large:

$$d\sigma_A(180^\circ) - d\sigma_A(0^\circ) \doteq 0.8\ e^2/m \ ;$$

however, there is an additional source of front-back assymmetry in the spin-dependent cross section $d\sigma_B$:

$$d\sigma_B(180^\circ) - d\sigma_A(0^\circ) \doteq 2.2\ (e^2/m) \ .$$

This spin-dependent asymmetry arises primarily from interference between the electric and magnetic scattering, which is dependent on the intrinsic and anomalous magnetic moments, and also on the mesonic structure effects.

The differential cross section at $k_\ell = 150$ Mev predicted by Capps and Holladay,[12] who use a modification of the weak pion-nucleon coupling theory of Sachs and Foldy,[13] is similar to the results of Section IIA in the forward direction, but increases only to about $d\sigma \approx 0.3\ e^2/m$ at $\theta = 180^\circ$. In this case the magnetic amplitudes are small; the principal effect of the proton's pionic structure is to reduce the magnitude of the electric dipole amplitudes from their threshold values. It is expected that the magnetic amplitudes are underestimated by this theory, however, since the scattering from the pionic contribution to the static magnetic moment is not included in such a weak-coupling calculation.

Inaccuracy of the results of Section IIA may arise from inaccuracy of either the structure-independent terms of the scattering amplitude (those terms depending on only the mass, charge, and anomalous magnetic moment) or the pionic-structure modification terms. An estimate of the inaccuracy of the structure-independent terms may be made by setting the functions $\mathcal{M}(k)$ and $\mathcal{E}(k)$ of Eqs. (11) equal to zero, and comparing

---

12 R. H. Capps and W. G. Holladay, Phys. Rev. 99, 931 (1955). The curve showing the effect of the inclusion of the anomalous magnetic moment in Fig. 2 of this reference is incorrectly computed; the resulting differential cross section should increase as the scattering angle increases.

13 R. G. Sachs and L. L. Foldy, Phys. Rev. 80, 824 (1950).

the resulting computed differential cross section with the cross section given by the Klein-Nishina formula modified by inclusion of a Pauli anomalous-moment term.[14] Such a comparison is given, for $k_\ell = 150$ Mev, in Fig. 5. It is seen that the neglect of certain recoil effects in the present model leads to an overestimation of the structure-independent differential cross section at angles other than forward angles of about 20%.

The assumption that the mesonic structure modifications are appreciable only in the amplitudes $T_{3/2}^{mg}$ and $T_{\frac{1}{2}}^{e\ell}$ leads to spin-dependent electric and magnetic amplitudes of large absolute value. This leads to a large backward peaking in the spin-dependent cross section. Figure 3 illustrates the effect of a different assumption concerning mesonic structure effects.

Because the choices of both structure-independent and structure-dependent effects in the present model tend to overestimate the cross section in the range $90^\circ < \theta < 180^\circ$, the curves of Figs. 2 and 4 probably are somewhat high in this region. In our opinion a reasonable guess would be that the curves in Figs. 2 and 4 are about $1\frac{1}{2}$ times too large at 180°.

---

[14] J. L. Powell, Phys. Rev. 75, 32 (1949).

III. SCATTERING FROM DEUTERONS

A. The Differential Cross Sections

Information concerning the scattering of photons from neutrons must be obtained from the results of scattering photons from complex nuclei. The results of scattering from complex nuclei may be related simply to the corresponding neutron and proton cross sections if the total nuclear scattering amplitude is approximately equal to the superposition of the scattering amplitudes from a group of free protons and neutrons having the same momentum distribution as the nucleons in the nucleus. This "impulse approximation" has been studied by Chew and others[7] and applied to many collision problems involving complex nuclei. The impulse assumption is necessary to the formulas given by Pugh, Frisch, and Gomez[1] for photon scattering from medium and heavy nuclei.

Because a deuteron consists of only two nucleons and because these nucleons have a relatively large average separation, deuterons represent favorable nuclei for application of the impulse approximation to a collision process. In this section the impulse approximation is used to predict the results of high-energy photon-deuteron scattering.

The formulas relating the deuteron amplitude to the proton and neutron amplitudes in the impulse approximation are similar to those given by Chew and Lewis for the photoproduction of neutral pions from deuterium[15] thus these formulas will be listed here without derivation. Letting $\mathcal{A}$ and $\mathcal{B}$ represent spin-independent and spin-dependent amplitudes, and letting the subscripts n and p refer to the neutron and proton amplitudes,

---

[15] G. F. Chew and H. W. Lewis, Phys. Rev. 84, 779 (1951).

respectively, we may write the unpolarized differential cross sections for scattering photons from free protons and free neutrons as

$$d\sigma_p = |\mathcal{A}_p|^2 + |\mathcal{B}_p|^2$$
$$d\sigma_n = |\mathcal{A}_n|^2 + |\mathcal{B}_n|^2 \quad . \tag{18}$$

The relation of the quantities $\mathcal{A}_{p,n}$ and $\mathcal{B}_{p,n}$ to the scattering angle and to the various electric and magnetic amplitudes is given in Appendix B. The expression for the differential cross section for elastic photon scattering from deuterons is analogous to Eq. (25) of Reference 15 and is given, in the notation of Eqs. (18), by

$$d\sigma_d^{\text{elastic}} = \left\{ |\mathcal{A}_p + \mathcal{A}_n|^2 + \tfrac{2}{3} |\mathcal{B}_p + \mathcal{B}_n|^2 \right\} S(q) \quad , \tag{19}$$

where q is the magnitude of the vector $\underset{\sim}{q}$, which represents the momentum transferred to the nucleons in the collision. The "sticking factor" $S(q)$ measures the probability that the deuteron remains bound after the collision; this factor may be determined from the deuteron wave function $\phi(\underset{\sim}{r})$ by the equations

$$S(q) = F^2(\tfrac{1}{2} q) \quad , \tag{20}$$

$$F(q) = \int d^3r \; e^{-i\underset{\sim}{q}\cdot\underset{\sim}{r}} \; \phi^2(\underset{\sim}{r}) \quad . \tag{21}$$

The sum of the differential cross sections for inelastic and elastic scattering is given by an expression analogous to Eq. (27) of Reference 15. Representing this sum by $d\sigma_d$, we have

$$d\sigma_d = |\mathcal{A}_p|^2 + |\mathcal{A}_n|^2 + |\mathcal{B}_p|^2 + |\mathcal{B}_n|^2 + 2\mathcal{A}_n^* \mathcal{A}_p F(q) + \tfrac{2}{3} \mathcal{B}_n^* \mathcal{B}_p F(q) \quad , \tag{22}$$

where the interference factor $F(q)$ is given by Eq. (21). In inelastic scattering the momentum transfer is not determined by the energy and scattering angle alone. In the present calculation this momentum transfer is assumed to be equal to the momentum transfer of the corresponding deuteron elastic scattering, an assumption which is accurate to order $k_\ell/2m$.

In order to compute the form factors $F(q)$ and $S(q)$ we assume that the deuteron wave function $\phi(\underset{\sim}{r})$ is given by the Hulthen function

$$\phi(\underset{\sim}{r}) = \left[\frac{\alpha\beta(\beta+\alpha)}{2\pi(\beta-\alpha)^2}\right]^{\frac{1}{2}} \frac{e^{-\alpha r} - e^{-\beta r}}{r} , \tag{23}$$

where the constants α and β are expressed in terms of the nucleon mass and the deuteron binding energy Y by the equations

$$\alpha = (Ym)^{\frac{1}{2}} \approx 0.322\mu ;$$

$$\beta = 6\alpha .$$

The factors $F(q)$ and $S(q)$ that result from this choice of $\phi(\underset{\sim}{r})$ are given as functions of the momentum transfer, by Chew.[16] They are both unity at $q = 0$, indicating that the scattering is completely coherent in the forward direction. As q increases the two functions decrease monotonically. That the difference between $F(q)$ and $S(q)$ is not too large for any value of q indicates that, if the neutron-proton system remains in a triplet state after the collision, the interference effect in the <u>inelastic</u> scattering is not too large. Thus if the momentum transfer is large enough

---

16 G. F. Chew, Phys. Rev. <u>84</u>, 710 (1951). See Eq. (5) and Fig. 1 of this paper.

to split the deuteron, the "struck" nucleon will generally be left with a kinetic energy noticeably larger than that of the other nucleon, in which case interference effects are small. If, on the other hand, the neutron-proton system is in a singlet state after the collision, the scattering must be inelastic; interference effects in such scattering may be important.

In order to make a definite prediction for the gamma-deuteron cross sections, we assume that the mesonic effects in photon-nucleon reactions are charge-symmetric, and contribute equally to the neutron and proton amplitudes. In such a model the neutron amplitude differs from the proton amplitude only in the effects of the total charge and the intrinsic magnetic moment. The neutron amplitudes $A_n^{e\ell}$, A_n^{mg}, $B_n^{e\ell}$, and B_n^{mg} are given, in terms of the corresponding proton amplitudes, by

$$\begin{aligned}
\frac{k_\ell}{k}\left(A_n^{e\ell} - A_p^{e\ell}\right) &= \frac{e^2}{m} , \\
\frac{k_\ell}{k}\left(A_n^{mg} - A_p^{mg}\right) &= 0 , \\
\frac{k_\ell}{k}\left(B_n^{e\ell} - B_p^{e\ell}\right) &= \frac{e^2}{2m^2}\,(2\lambda + 1) , \\
\frac{k_\ell}{k}\left(B_n^{mg} - B_p^{mg}\right) &= -\frac{e^2}{2m^2}\,(2\lambda + 1) .
\end{aligned} \tag{24}$$

Thus, the structure-independent parts of the neutron amplitudes are given by

$$A_n^{mg} = A_n^{e\ell} = B_n^{e\ell} = 0 ;$$

$$B_n^{mg} = e^2 \lambda^2 k/2m^2 .$$

The difference between the anomalous moments of the proton and neutron is neglected here.

If the proton amplitudes are determined by the procedure of Section IIA (neglect of mesonic structure modifications in $T_{3/2}^{e\ell}$ and $T_{\frac{1}{2}}^{mg}$, and use of dispersion relations), and the neutron amplitudes are determined by Eqs. (24), the resulting deuteron elastic and inelastic cross sections may be computed from Eqs. (19) and (22) and the formulas given in Appendix B. The resulting differential cross sections, converted to the laboratory system, are shown at three energies in Figs. 6 and 7.

B. Accuracy of the Model

At present we know of no reliable experiment that may be used to check the present results for photon-deuteron scattering. Such measurements may be made in the near future, however; therefore it is important to estimate the accuracy of the approximations used here.

It is expected that the deuteron cross sections of Figs. 6 and 7 are overestimated somewhat at backward angles for the same reasons as given in Section IIB in the discussion of the proton cross section. Furthermore, there are several sources of error in the present treatment of photon-deuteron scattering in addition to those which are present in the treatment of Section II of photon-proton scattering. One such source is the internal momentum of the deuteron; because of this momentum the relative energy between the photon and the "struck" nucleon is not fixed by the gamma-ray energy alone. The impulse approximation can be accurate only if the resulting spread in relative energy is small enough so that the scattering amplitude does not vary by a large amount within the range of the spread. If the deuteron wave function is given by Eq. (23), a calculation shows that,

for an incident gamma energy of 150 Mev, the spread in gamma-nucleon relative energy is around 15 Mev; that is, 80% of the time the relative gamma-nucleon energy is within 7.5 Mev of the corresponding energy for a nucleon at rest. From the curves of Fig. 7 it appears that the differential cross section at some fixed angle may vary by as much as 0.4 e^2/m in 7.5 Mev. Therefore errors from this source are not negligible.

The neglect of recoil leads to several types of small errors in the model. The effect of nucleon recoil in the gamma scattering from the nucleon's pionic structure leads to violations of the charge-symmetry assumption, of order μ/m. Experiments on the closely related process of charged pion production by photons on deuterium indicate that the violation of charge symmetry in this process is of the expected order, about 15%.[17] The assumption that the momentum transferred to the nucleons in inelastic scattering is equal to the momentum transfer of the corresponding elastic scattering is another source of recoil errors, which, in this case, are of order $k_\ell/2m$.

The impulse assumption, that the neutron and proton amplitudes are additive, neglects the effect of "co-operation" between the nucleons in the photon scattering. We may estimate the magnitude of these effects by making use of certain experimental data. In order to formulate this estimate we write the amplitude T_{df} for elastic forward scattering from deuterons in a form that is somewhat similar to that of Eq. (1),

$$T_{df}(k) = A_d(k)\, \underset{\sim}{e}\cdot\underset{\sim}{e}' + B_d(k)(\underset{\sim}{\sigma}_p + \underset{\sim}{\sigma}_n)\cdot \underset{\sim}{e} \times \underset{\sim}{e}' + \text{other terms}, \qquad (25)$$

where $\underset{\sim}{\sigma}_p$ and $\underset{\sim}{\sigma}_n$ are the spin operators for the proton and neutron, respectively. The coherent amplitude A_d may be written in terms of the

[17] Sands, Teasdale, and Walker, Phys. Rev. 96, 849 (1954).

corresponding proton and neutron amplitudes by the equation

$$A_d(k) = A_p(k) + A_n(k) + \Delta(k) \quad . \tag{26}$$

The quantity $\Delta(k)$ is zero in the impulse approximation and represents the error in A_d due to the impulse assumption. The imaginary part of Δ may be estimated from experimental data, if use is made of the optical relations,

$$\begin{aligned} \mathrm{Im}\, A_p &= (k/4\pi)\sigma_{\pi p} \quad , \\ \mathrm{Im}\, A_n &= (k/4\pi)\sigma_{\pi n} \quad , \\ \mathrm{Im}\, A_d &= (k/4\pi)(\sigma_{\pi d} + \sigma_{dis}) \quad . \end{aligned} \tag{27}$$

The cross sections $\sigma_{\pi p}$, $\sigma_{\pi n}$, and $\sigma_{\pi d}$ represent the total cross sections for photoproduction, by unpolarized photons, of pions from protons, neutrons, and deuterons, respectively, while σ_{dis} represents the corresponding cross section for photodisintegration of deuterons. Only terms of order e^2 are included in Eqs. (27).

If Eqs. (27) are combined with Eq. (26), the following expression for the imaginary part of $\Delta(k)$ is obtained:

$$\mathrm{Im}\ \Delta(k) = (k/4\pi)\left[\sigma_{\pi d}(k) - \sigma_{\pi p}(k) - \sigma_{\pi n}(k)\right] + (k/4\pi)\sigma_{dis}(k). \tag{28}$$

The two terms on the right side of this expression are treated here as separate corrections. The quantity $\sigma_{\pi d}(k) - \sigma_{\pi p}(k) - \sigma_{\pi n}(k)$ is zero for $k_\ell < 140$ Mev; it is not known at energies above pion-production threshold, since $\sigma_{\pi n}$ is not known. However, there is evidence that the

π^+ photoproduction ratio of deuterium to hydrogen in the energy range under consideration here is about 0.9, suggesting that the ratio $\left| (\sigma_{\pi d} - \sigma_{\pi p} - \sigma_{\pi n}) \right| / \sigma_{\pi d}$ is probably not large, perhaps about 10% or 15%.[18] That part of Im Δ resulting from photodisintegration, $(k/4\pi)\sigma_{dis}$, is finite at all but very low energies. For photon energies in the range 100 to 200 Mev, however, $(k/4\pi)\sigma_{dis}$ is not greater than 0.30 e^2/m. Thus, in this energy range, the quantity Im Δ probably is not more than 0.3 or 0.35 e^2/m.

The real part of $\Delta(k)$ also may be estimated, if use is made of dispersion relations. The real parts of A_d and A_n satisfy dispersion relations which are analogous to the relation for A_p, Eq. (5). If the dispersion equations for $A_n(k)$ and $A_p(k)$ are subtracted from the equation for $A_d(k)$, the result is an equation for Re $\Delta(k)$,

$$\frac{k_\ell}{k} \operatorname{Re} \Delta(k) = \frac{e^2}{2m} + \frac{k^2}{2\pi^2} P \int_0^\infty dk_\ell' \frac{\sigma_{dis}(k') + \left[\sigma_{\pi d}(k') - \sigma_{\pi p}(k') - \sigma_{\pi n}(k')\right]}{(k_\ell'^2 - k_\ell^2)} \tag{29}$$

The constant $e^2/2m$ results from the difference of the threshold values for scattering from deuterons and from protons.

Again we make the estimate that the error that arises because $\sigma_{\pi d} - \sigma_{\pi p} - \sigma_{\pi n}$ is not zero is probably not much more than 15%.

---

18 Crowe, Friedman, and Hagerman, Phys. Rev. 100, 1799 (1956).

In order to determine the contribution to Re Δ from virtual photodisintegration of deuterons, we neglect the difference between $\sigma_{\pi d}$ and $\sigma_{\pi p} + \sigma_{\pi n}$, and evaluate the integral in Eq. (29) from the experimental data on photodisintegration. The result is not very energy-dependent in the range 100 Mev $< k_\ell <$ 200 Mev and is given approximately by,

$$1.08 \text{ Re } \Delta(k) \approx 0.50\ (e^2/m) - 0.64\ (e^2/m) \approx -0.14\ (e^2/m) .$$

If the contributions to Re $\Delta(k)$ from the two sources--virtual pion production and virtual photodisintegration--are added together, it is seen that $|\text{Re } \Delta(k)|$ probably is not more than $0.2\ (e^2/m)$.

That the contribution to Re $\Delta(k)$ from virtual photodisintegration is fairly small (for $k_\ell >$ 100 Mev), may be understood more clearly if the region of integration of Eq. (29) is divided into two regions $k_\ell' >$ 100 Mev and $k_\ell' <$ 100 Mev. The contribution of $\sigma_{dis}(k')$ is small in the high-energy region, since the ratio $\sigma_{dis}/\sigma_{\pi d}$ is less than 0.25 throughout this region. In the low-energy region, the photodisintegration cross section is large, $\sigma_{dis} \approx 10^{-27}$ cm^2, and is primarily the result of spin-independent, electric dipole transitions. For this region the energy denominator $(k_\ell'^2 - k_\ell^2)^{-1}$ may be expanded in powers of $(k_\ell'^2/k_\ell^2)$ so that the low-energy contribution to the right side of Eq. (29) is

$$\frac{e^2}{2m} - \frac{1}{2\pi^2} \int_0^{100\text{ Mev}} dk_\ell'\, \sigma_{dis}(k) \left(1 + \frac{k_\ell'^2}{k_\ell^2} + \frac{k'^4}{k^4} + \cdots\right) \qquad (30)$$

The zero-order term in this expansion, $(2\pi^2)^{-1} \int dk_\ell'\, \sigma_{dis}(k')$, is approximately equal to $0.59\ (e^2/m)$; thus it is nearly canceled by the threshold constant, $0.50\ (e^2/m)$. This is a rough restatement of the well-known f-sum rule for the deuteron, which states that the total

energy integral of the electric dipole cross section is approximately $0.5\ e^2/m$.[19] This fact has been pointed out by GGT, who show that the assumption that the impulse approximation is valid in the high-energy limit may be used to derive a sum rule for the total photodisintegration cross sections for complex nuclei.

The contribution to Eq. (30) from terms of higher order in $(k_\ell'^2/k_\ell^2)$ is small also, since $(k_\ell'^2/k_\ell^2)$ is small if k_ℓ' is such that $\sigma_{dis}(k')$ is large.

It is concluded that the quantities Re $\Delta(k)$ and Im $\Delta(k)$, which measure the inaccuracy of the impulse assumption, probably are not larger than 0.2 or 0.3 e^2/m. It may be argued further that similar corrections to both the spin-dependent and spin-independent amplitudes should be of this order or smaller at all angles. Experiments indicate that the deuteron-proton ratios for photoproduction of positive pions, and of neutral pions, do not vary much with angle; it appears that the impulse approximation is reasonably accurate for the process of photopion production at all angles.[18,20] Therefore that part of photon-deuteron scattering which proceeds through virtual pion production states may be treated by the impulse approximation fairly accurately for all scattering angles.

Similar arguments may be given for the contribution of virtual photodisintegration states. The fact that the total photodisintegration

---

[19] This sum rule is discussed by J. S. Levinger and H. A. Bethe, Phys. Rev. 78, 115 (1950).

[20] G. Cocconi and A. Silverman, Phys. Rev. 88, 1230 (1952); and Bingham, Keck, and Tollestrup, Phys. Rev. 98, 1187 (A) (1955).

cross section is small for energies greater than 100 Mev indicates that all partial-wave photodisintegration cross sections are small in this energy range; therefore the contributions to the deuteron-scattering differential cross sections from excitation of high-energy photodisintegration states should not be large at any angle. Excitation of low-energy photodisintegration states is primarily a spin-independent electric dipole process which, as shown above, gives corrections to the spin-independent electric dipole amplitude $A_d^{e\ell}$, which are of order

$$(2\pi^2)^{-1} \int_0^{100\,\mathrm{Mev}} \sigma_{dis}(k') \left[k_\ell'^{\,2}/k_\ell^{\,2} \right] dk_\ell' \approx 0.05\, e^2/m \quad .$$

It is concluded that the present model is not a precise one; errors due to neglect of certain recoil effects and errors due to neglect of effects in which the neutron and proton "cooperate" may lead to sizeable errors in the predicted photon-deuteron differential cross sections. Roughly speaking, at any given angle, these errors may be as large as $0.5\ e^2/m$ or so. Furthermore, we expect the predicted cross sections to be somewhat high for backward scattering angles for the reasons discussed in Section IIB. However, one may expect the predictions of this model to reveal the salient features of the actual cross sections, provided that the basic assumptions of the model are correct.

IV. POSSIBLE PHOTON-DEUTERON SCATTERING EXPERIMENTS

Because of the presence of the neutron-proton force, the present model is not expected to predict photon-deuteron scattering as accurately as scattering from free protons. However the difficulties of using photon-deuteron experiments to investigate the photon-nucleon interaction are partially compensated by one advantage of such experiments, namely the possibility of measuring several different quantities when the scattering is from deuterium. One can measure both the elastic and inelastic cross sections, and it may be possible to obtain further useful information by detecting the recoil of one of the nucleons in the inelastic photon-deuteron scattering.

In order to separate the elastic and inelastic scattering with present experimental equipment, one must detect the recoiling nucleon or deuteron in coincidence with the gamma ray, using a dectector that differentiates between deuterons, protons, and neutrons. Such a coincidence measurement is not too difficult in elastic scattering, since the recoil energy and angle of the deuteron are fixed by the incident energy and photon scattering angle. If the scattering is inelastic, however, the recoil of the nucleons is not fixed by the incident energy and photon scattering angle. For this reason the least difficult way to measure the inelastic cross section is to measure the total cross section and the elastic cross section and find the difference.

It is possible that still further information may be obtained from such coincidence experiments. If the impulse approximation is a fairly accurate description of the inelastic scattering, one expects that the nucleon which is "struck" by the photon has a high probability of recoiling

in a direction that is fairly close to the recoil direction in the corresponding scattering from free nucleons. If one can detect the recoiling "struck" nucleon with appreciable efficiency, one may obtain the ratio of knocked-out protons to knocked-out neutrons. In the impulse approximation this ratio is the ratio of the proton and neutron differential cross sections at the angle in question. Such a procedure is difficult experimentally, but has the advantage that a neutron-proton ratio is being determined; hence, the use of the impulse approximation in determining the free-particle cross-section ratio is free from some of the errors involved in the analysis of Section III.

We may make a rough estimate of the variation in direction of emission of the knocked-out nucleons by using the impulse approximation and assuming that the internal momentum spectrum of the deuteron is given by the Fourier transform of the expression for $\phi_0(\underset{\sim}{r})$ given in Eq. (23). For values of the incident photon energy and photon scattering angle of 140 Mev and 90° such as estimate indicates that in 50% or more of the inelastic collisions the knocked-out nucleon emerges in a cone of radial angle 18°, the center of this cone being very close to the direction of recoil in the corresponding scattering from free nucleons. Though such a cone is not small, it does appear possible to detect a reasonable proportion of the knocked-out nucleons. The efficiency of such a measurement would be lower than in an ordinary photon-scattering experiment, but it may not be as much lower as it would appear at first sight, for the following reason: Present-day photon scattering experiments are performed with bremmstrahlung beams having a wide energy spectrum, and the energy resolution of present gamma detectors is not very sharp. If the energy of the recoiling particle is measured, this measurement makes it easier to subtract events resulting from photons

in the low-energy tail of the bremmstrahlung spectrum. Furthermore, nucleons struck by low-energy photons have less chance of being knocked out of the deuteron and emitted in a direction inside a fairly small cone than do nucleons struck by high-energy photons.

V. CONCLUSIONS

The development of dispersion relations has made it possible to predict many features of photon-nucleus scattering from a knowledge of photopion-production cross sections. In the work presented here two dispersion relations, together with several reasonable approximations, are used to predict the differential cross sections for photon-proton scattering and elastic and inelastic photon-deuteron scattering at energies less than 200 Mev. At present the experimental data are not accurate enough to check the model used here.

Since the photon scattering amplitudes may be expressed approximately in terms of photopion-production cross sections, the primary purpose of measuring photon-nucleon scattering probably is not to find new information concerning the pionic structure of nucleons, but rather to test presently accepted ideas, such as the dispersion relations, and the assumption that only S-wave and P-wave pions are important to an understanding of low-energy pion-nucleon phenomena. These two assumptions are basic to the present model. Further approximations are made (such as the impulse approximation), but the accuracy of these further approximations is estimated. If the measured cross sections should differ from those predicted in Sections II and III by amounts much larger than expected, this probably would indicate the failure of one of the two basic assumptions.

In the present model effects of virtual transitions of the nucleons to a nucleon-pion P-wave state of angular momentum 3/2 (the resonant state) are important, but they do not dominate the effects of S-wave pion-nucleon states, at least at energies below 200 Mev. As the photon

energy increases from 120 to 300 Mev, the virtual P-wave, $j = 3/2$, pion-nucleon state becomes more and more important. Compton scattering at energies corresponding to the peak of the resonance in this state (photon energies in the range 275 to 350 Mev) is not treated here, but this problem is interesting, both experimentally and theoretically. In this region the imaginary part of the amplitudes should be quite large; it is easily shown from Eq. (4) that the imaginary part of the spin-independent forward amplitude, $\mathrm{Im}\, A_p(k)$, is a high as $3\, e^2/m$ at the peak of the resonance. If only electric and magnetic dipole waves contribute to $A_p(k)$, the condition $\mathrm{Im}\, A_p(k) \approx 3\, e^2/m$ implies that the total scattering cross section is at least $4\frac{1}{2}$ times the Thomson cross section; thusthe total photon-proton cross section must be relatively large in the resonance region.

ACKNOWLEDGMENTS

The author wishes to thank Larry Higgins for many helpful discussions concerning photon scattering, and Joan Capps for helping with the numerical calculations.

This work was performed under the auspices of the U.S. Atomic Energy Commission.

APPENDIX A: CONSEQUENCES OF UNITARITY

Equations of the type of Eqs. (4) and (13) may be derived simply from the unitarity property of the scattering matrix. Since the photon-nucleon scattering problem is more complicated than some others because of the spins of the particles, we indicate in this appendix how the numerical coefficients of Eqs. (4) and (13) are obtained.

Let the plane wave that represents the incoming wave plus the unscattered outgoing wave for a particular polarization state in a two-particle scattering problem be expanded in spherical waves in the following manner,

$$\psi^{\alpha}(s)\, e^{ik\cdot r} = \sum_i C_i^{\alpha}\, \chi_i(\theta, s)\, f_i(kr) \quad , \tag{A1}$$

where $\psi^{\alpha}(s)$ represents the spin wave functions of the particles in the polarization state denoted by α , $\chi_i(\theta, s)$ represents a normalized "angular" wave function depending on orbital and spin angular momenta, and $f_i(kr)$ is the radial wave function depending on the relative particle separation r , normalized so that, as $r \to \infty$, $f_i(kr) \approx \frac{\sin kr}{kr}$. The complex numbers C_i^{α} are the expansion constants. Let the states denoted by the index i be eigenstates of the scattering in the sense that the scattering cannot cause transitions between states corresponding to different values of i (though final states involving different particles may be produced). It may be easily shown from the unitarity of the S matrix that the imaginary parts of the scattering amplitudes T_i (defined in terms of the complex phase shifts δ_i by the relation $T_i = (e^{i\delta_i} \sin\delta_i)/k$) are related to partial cross sections by the equation

$$\sigma_i^{\alpha} = \frac{\left| C_i^{\alpha} \right|^2}{k} \operatorname{Im} T_i \quad , \tag{A2}$$

where σ_i^{α} is the partial cross section (including elastic and inelastic processes) corresponding to the spherical wave state i for an incident beam of polarization α.

In the present model the index i refers to the four dipole amplitudes discussed in Section II, $T_{3/2}^{e\ell}$, $T_{3/2}^{mg}$, $T_{\frac{1}{2}}^{e\ell}$, and $T_{\frac{1}{2}}^{mg}$. If we quantize along the direction of the incident beam there are two polarization states which may scatter differently, the state in which the nucleon and photon spins are parallel, and the antiparallel state. (Reversing the direction of both spins simultaneously does not affect the scattering cross section.) We denote these two states by the superscripts p and a. If use is made of Clebsch-Gordon coefficients and the expansion in vector spherical harmonics given in Blatt-Weisskopf[21], it may be seen that the constants $\left|C_i^{\alpha}\right|^2$ in the present model are given by

$$\begin{aligned}
\left| C_{3/2,e\ell}^{\;p} \right|^2 &= \left| C_{3/2,mg}^{\;p} \right|^2 = 6\pi , \\
\left| C_{\frac{1}{2},e\ell}^{\;p} \right|^2 &= \left| C_{\frac{1}{2},mg}^{\;p} \right|^2 = 0 , \\
\left| C_{3/2,e\ell}^{\;a} \right|^2 &= \left| C_{3/2,e\ell}^{\;a} \right|^2 = 2\pi , \\
\left| C_{\frac{1}{2},e\ell}^{\;a} \right|^2 &= \left| C_{\frac{1}{2},e\ell}^{\;a} \right|^2 = 4\pi .
\end{aligned} \tag{A3}$$

From Eqs. (A2) and (A3), equations for the partial cross sections may be obtained.

---

21 J. M. Blatt and V. F. Weisskopf, Theoretical Nuclear Physics, John Wiley and Sons, Inc., New York, 1952, Appendices A and B.

An unpolarized photon-nucleon beam may be considered as the sum of a parallel polarized and an antiparallel polarized beam, occurring with equal intensity. Consequently an unpolarized partial cross section σ_i is given in terms of the partial cross sections σ_i^p and σ_i^a by the equation

$$\sigma_i = \tfrac{1}{2}(\sigma_i^p + \sigma_i^a) \quad . \tag{A4}$$

Combining Eqs. (A2), (A3), and (A4), we obtain the relations for the electric amplitudes,

$$\begin{aligned} \mathrm{Im}\ T_{3/2}^{e\ell} &= (k/4\pi)\sigma_{3/2,e\ell} \quad , \\ \mathrm{Im}\ T_{\frac{1}{2}}^{e\ell} &= (k/2\pi)\sigma_{\frac{1}{2},e\ell} \quad . \end{aligned} \tag{A5}$$

If Eqs. (A5) are combined with the expressions for $A^{e\ell}$ and $B^{e\ell}$, Eqs. (7), the following equations result:

$$\begin{aligned} \mathrm{Im}\ A^{e\ell} &= (k/4\pi)(\sigma_{3/2,e\ell} + \sigma_{\frac{1}{2},e\ell}) \quad , \\ \mathrm{Im}\ B^{e\ell} &= (k/4\pi)(\tfrac{1}{2}\sigma_{3/2,e\ell} - \sigma_{\frac{1}{2},e\ell}) \quad . \end{aligned} \tag{A6}$$

Exactly similar relationships hold for the magnetic amplitudes. Adding together the electric and magnetic amplitudes (see Eqs. (8)) and using the fact that the total cross section is the sum of partial cross sections, one obtains Eqs. (4) and (13) of Section II.

APPENDIX B:

RELATION OF VARIOUS AMPLITUDES TO DIFFERENTIAL CROSS SECTIONS

In this appendix the amplitudes $\mathcal{A}_p$, $\mathcal{A}_n$, $\mathcal{B}_p$ and $\mathcal{B}_n$ of Eqs. (18), (19), and (22) are related to the scattering angle and to the amplitudes $A_{p,n}^{e\ell}$, $A_{p,n}^{mg}$, etc. Formulas for the differential cross sections in different states of polarization of the photons and the target may be derived by the standard method of expanding the photon waves in vector spherical harmonics.[21] Since the scattering cross sections discussed in this work refer to the case of no polarization, we shall list here differential cross section formulas only for unpolarized beams. Such formulas are comparatively simple since the spin-independent amplitudes and spin-dependent amplitudes cannot interfere for "unpolarized" scattering. We introduce four angular dependent functions $X_A^{e\ell}$, X_A^{mg}, $X_B^{e\ell}$, and X_B^{mg} (which are related to combinations of the vector spherical harmonics), and express the amplitudes $\mathcal{A}_{p,n}$ and $\mathcal{B}_{p,n}$ in the form

$$\begin{aligned}
\mathcal{A}_p &= A_p^{e\ell} X_A^{e\ell} + A_p^{mg} X_A^{mg} , \\
\mathcal{B}_p &= B_p^{e\ell} X_B^{e\ell} + B_p^{mg} X_B^{mg} , \\
\mathcal{A}_n &= A_n^{e\ell} X_A^{e\ell} + A_n^{mg} X_A^{mg} , \\
\mathcal{B}_n &= B_n^{e\ell} X_B^{e\ell} + B_n^{mg} X_B^{mg} .
\end{aligned} \tag{B1}$$

In order to compute the cross sections of Eqs. (18), (19), and (22), one may substitute for $\mathcal{A}_{p,n}$ and $\mathcal{B}_{p,n}$ the above expressions and make use of the relations

$$\left| X_A^{e\ell} \right|^2 = \left| X_A^{mg} \right|^2 = \tfrac{1}{2}(1 + \cos^2 \Theta) \quad ,$$

$$\left| X_B^{e\ell} \right|^2 = \left| X_B^{mg} \right|^2 = \tfrac{1}{2}(3 - \cos^2 \Theta) \quad , \tag{B2}$$

$$X_A^{e\ell *} X_A^{mg} = X_B^{e\ell *} X_B^{mg} = \cos \Theta \quad .$$

The angular functions given above are determined by taking the sum and average of final and initial polarization directions of the dipole photon waves involved in the present model.

If, for example, the above procedure is applied to the scattering from protons, one obtains

$$\begin{aligned} d\sigma_p &= \left|\mathcal{A}_p\right|^2 + \left|\mathcal{B}_p\right|^2 \\ &= \left(\left| A_p^{e\ell} \right|^2 + \left| A_p^{mg} \right|^2 \right) \tfrac{1}{2}(1 + \cos^2 \Theta) \\ &\quad + \left(\left| B_p^{e\ell} \right|^2 + \left| B_p^{mg} \right|^2 \right) \tfrac{1}{2}(3 - \cos^2 \Theta) \\ &\quad + (A_p^{e\ell *} A_p^{mg} + B_p^{e\ell *} B_p^{mg})\, 2 \cos \Theta \quad . \end{aligned} \tag{B3}$$

The above formulas represent a shorthand method of writing the cross sections discussed in this paper. For a derivation of the form of the scattering amplitude, the reader is referred to References 5 and 21. The appendix of Reference 5 gives the form of the photon-nucleon scattering cross sections for different states of polarization.

FIGURE CAPTIONS

Figure 1: Values of the amplitudes $\mathcal{E}$ and $\mathcal{M}$ as functions of the incident photon energy (laboratory system) The solid lines represent the real parts of the amplitudes; the dashed lines represent the imaginary parts.

Figure 2: Calculated photon-proton differential cross sections in the center-of-mass system, shown at incident photon energies in the laboratory system of 120, 150, and 185 Mev.

Figure 3: Dependence of the calculated photon-proton center-of-mass differential cross section on the value assumed for the pionic structure modification of the amplitude $T_{3/2}^{e\ell}$. The ratio R is defined in Eq. (17). The curves refer to an incident photon energy in the laboratory system of 150 Mev.

Figure 4: Calculated photon-proton differential cross sections in the laboratory system.

Figure 5: Comparison of the structure-independent part of the calculated photon-proton differential cross section to the cross section calculated from the Klein-Nishina formula modified by the inclusion of a Pauli anomalous-moment term. The Klein-Nishina cross section $d\sigma_{KN}$ is taken from Reference 14. The cross section $d\sigma_{SI}$ results from setting $\mathcal{E}$ and $\mathcal{M}$ equal to zero in the present model. The quantities are measured in the laboratory system, at an incident photon energy of 150 Mev.

FIGURE CAPTIONS (Cont.)

Figure 6: Calculated photon-deuteron differential elastic cross sections in the laboratory system.

Figure 7: Calculated photon-deuteron differential cross sections in the laboratory system. These curves represent the sums of the elastic and inelastic scattering cross sections.

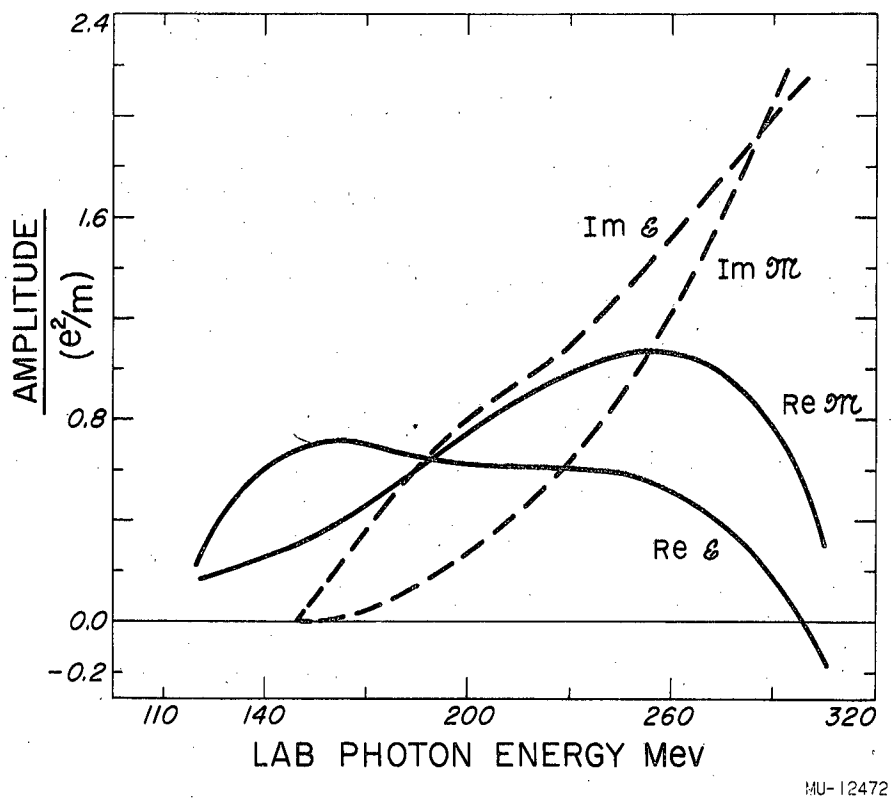
2.4
1.6
0.8
0.0
-0.2
AMPLITUDE
(e²/m)
Im 𝒢
Im 𝔐
Re 𝔐
Re 𝒢
110
140
200
260
320
LAB PHOTON ENERGY Mev
MU-12472

Fig. 1

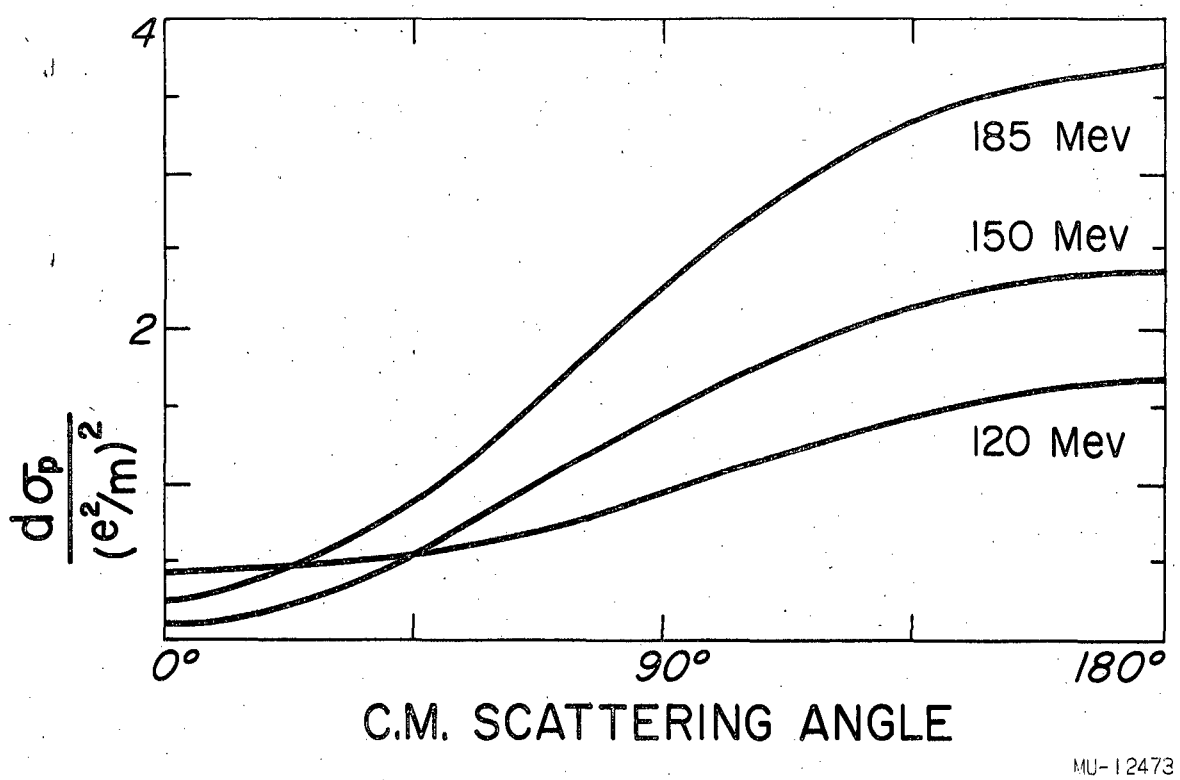
4
2
185 Mev
150 Mev
120 Mev
$\frac{d\sigma_p}{(e^2/m)^2}$
0°
90°
180°
C.M. SCATTERING ANGLE
MU-12473

Fig. 2

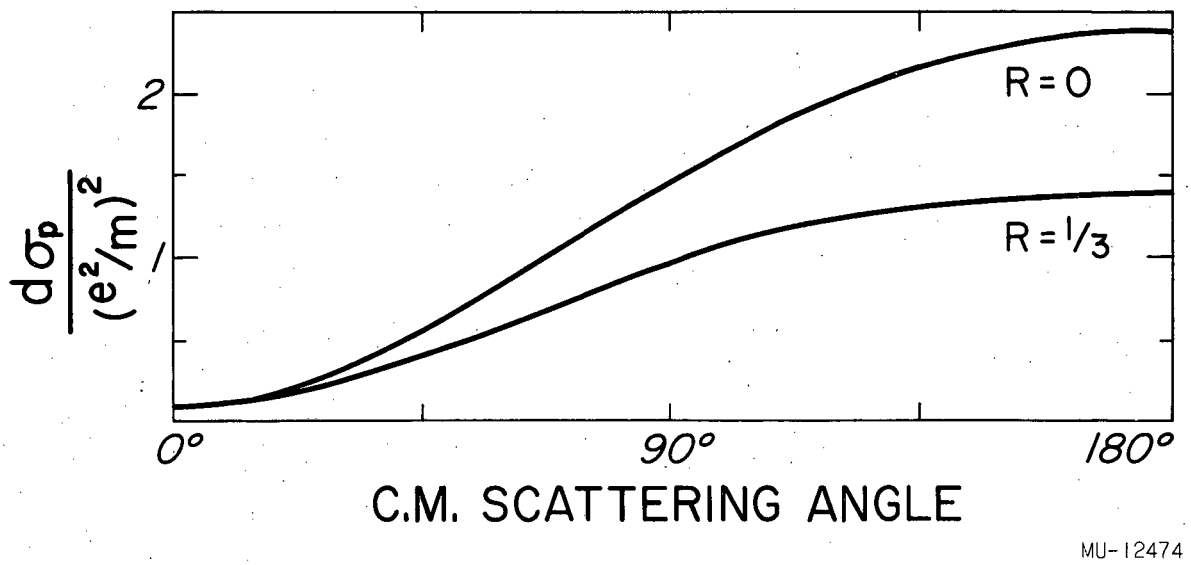
2
1
$\frac{d\sigma_p}{(e^2/m)^2}$
R = 0
R = 1/3
0°
90°
180°
C.M. SCATTERING ANGLE
MU-12474

Fig. 3

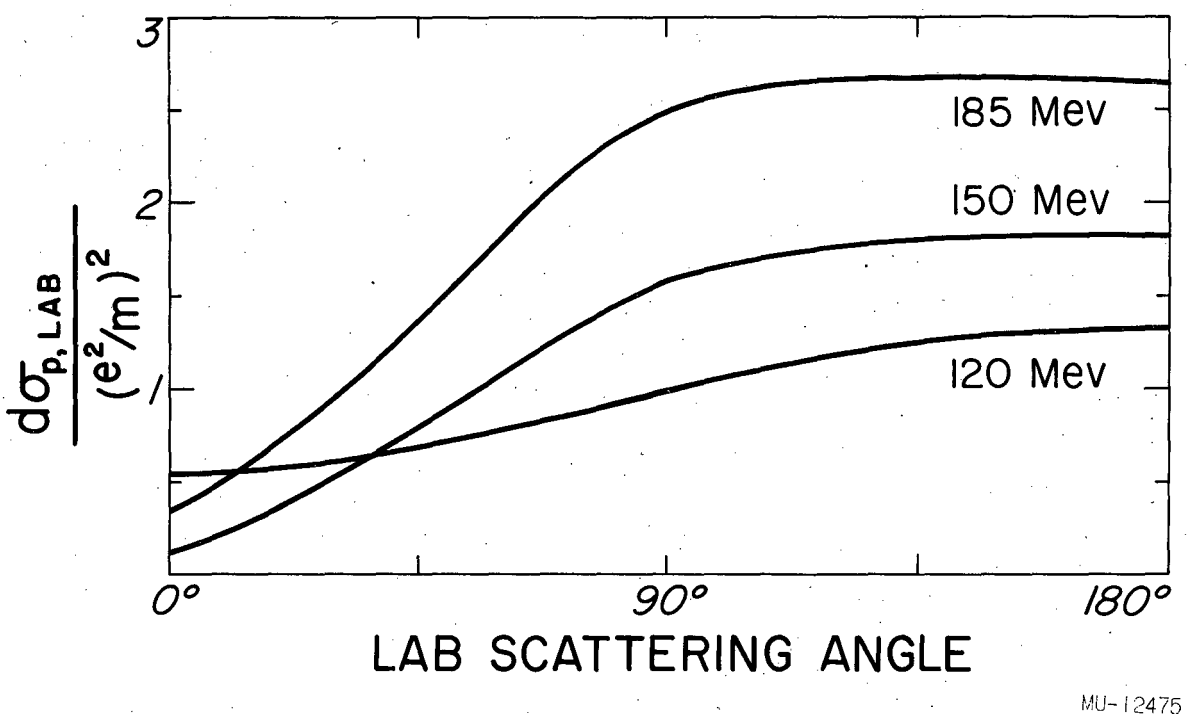
3
2
1
185 Mev
150 Mev
120 Mev
$\frac{d\sigma_{p,LAB}}{(e^2/m)^2}$
0°
90°
180°
LAB SCATTERING ANGLE
MU-12475

Fig. 4

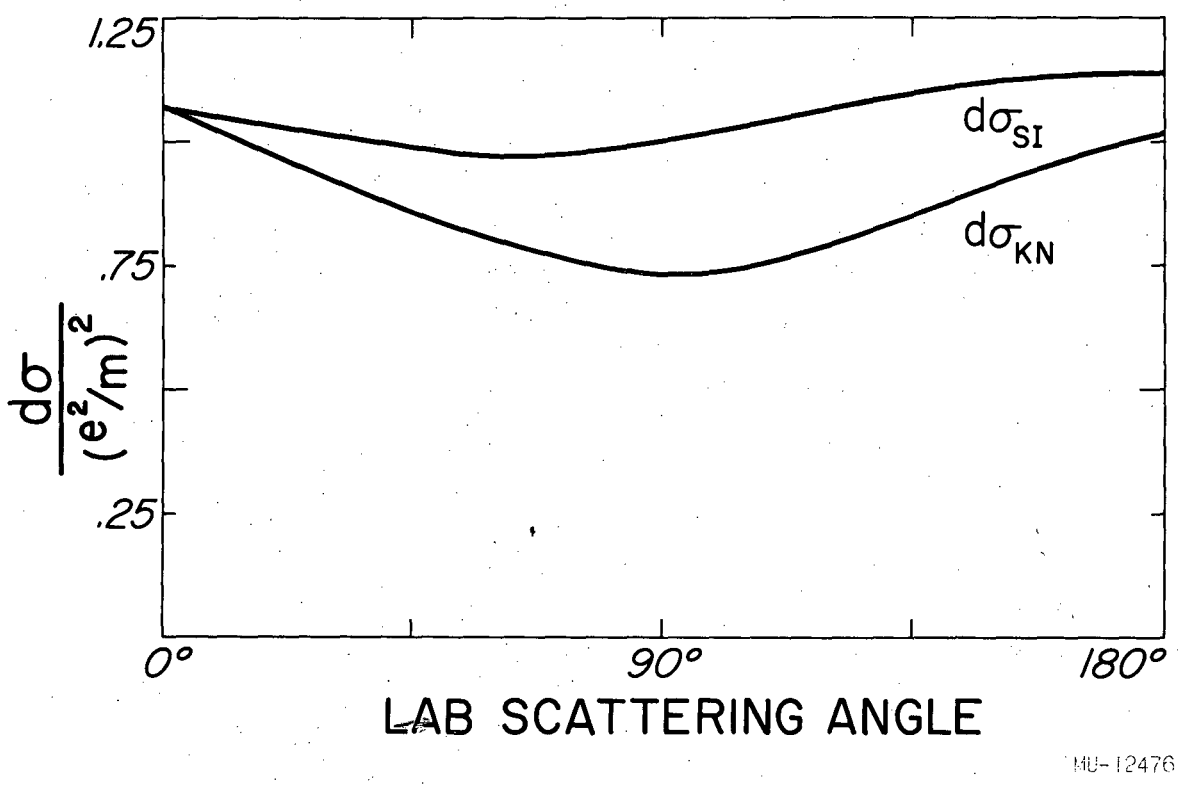
1.25
.75
.25
$\frac{d\sigma}{(e^2/m)^2}$
$d\sigma_{SI}$
$d\sigma_{KN}$
0°
90°
180°
LAB SCATTERING ANGLE
MU-12476

Fig. 5

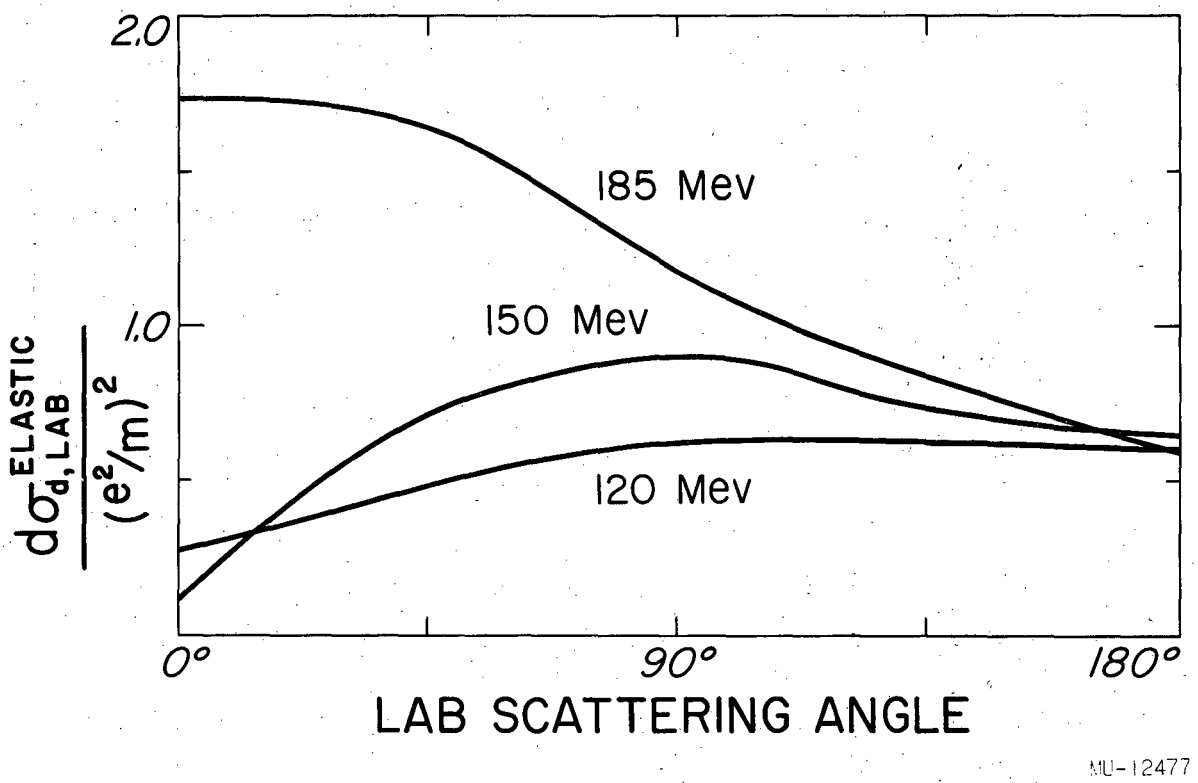
2.0
1.0
185 Mev
150 Mev
120 Mev
$\frac{d\sigma_{d,LAB}^{ELASTIC}}{(e^2/m)^2}$
0°
90°
180°
LAB SCATTERING ANGLE
MU-12477

Fig. 6

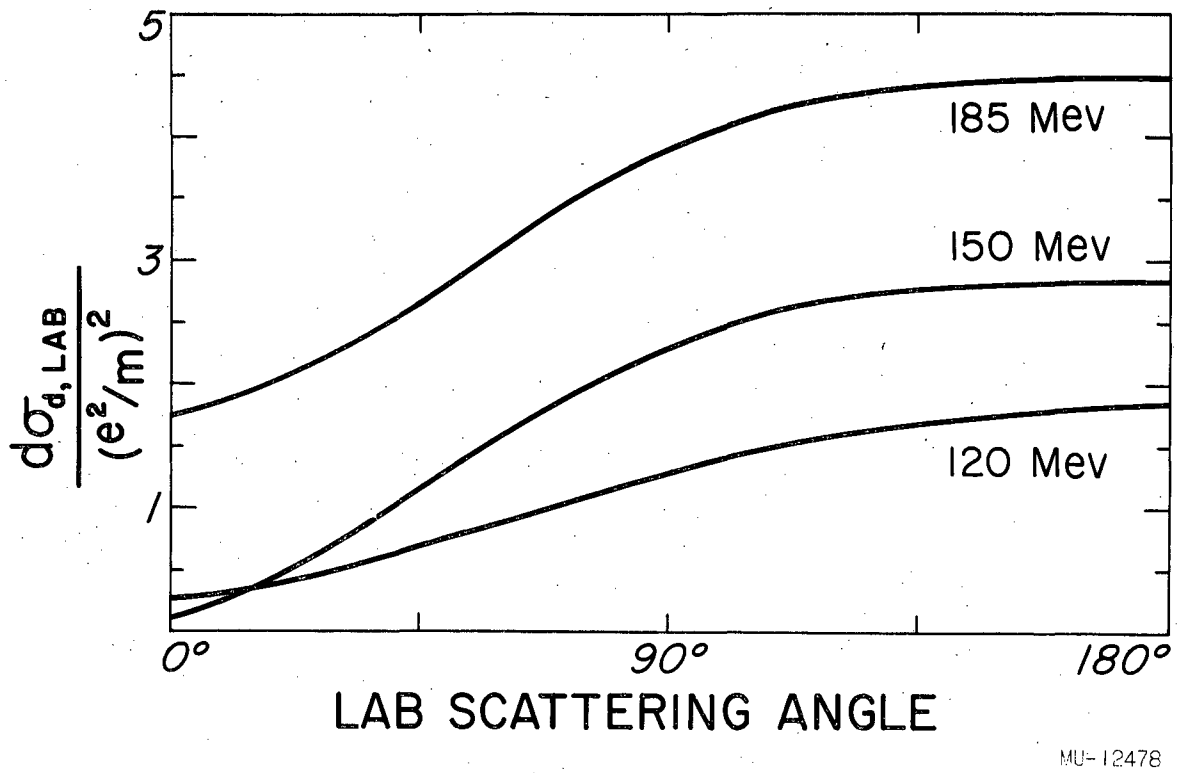
5
3
1
185 Mev
150 Mev
120 Mev
$\frac{d\sigma_{d,LAB}}{(e^2/m)^2}$
0°
90°
180°
LAB SCATTERING ANGLE
MU-12478

Fig. 7